J|A|C|S ARTICLES

Published on Web 01/26/2009

Reversible Lability by *in Situ* Reaction of Self-Assembled Monolayers

Héctor M. Saavedra, Christopher M. Thompson, J. Nathan Hohman, Vincent H. Crespi, and Paul S. Weiss*

Departments of Chemistry and Physics, The Pennsylvania State University, 104 Davey Laboratory, University Park, Pennsylvania 16802

Received September 29, 2008; E-mail: stm@psu.edu

Abstract: We describe a new methodology for the fabrication of controllably displaceable monolayers using a carboxyl-functionalized self-assembled monolayer and *in situ* Fischer esterification, a simple and reversible chemical reaction. Using an 11-mercaptoundecanoic acid monolayer as a model system, we show that *in situ* esterification results in the creation of subtle chemical and structural defects. These defects promote molecular exchange reactions with *n*-dodecanethiol molecules, leading to the complete and rapid displacement of the exposed areas. Displacement results in well-ordered crystalline *n*-dodecanethiolate monolayer films. We also show that the complementary hydrolysis reaction can be employed to quench the reacted monolayer, significantly hindering further displacement. The generality of reversible lability was tested by applying the *in situ* esterification reaction to the structurally distinct carboxyl-functionalized molecule 3-mercapto-1-adamantanecarboxylic acid. Beyond its applicability to create mixed-composition monolayers, this methodology could be combined with chemical patterning techniques, such as microdisplacement printing, to fabricate complex functional surfaces.

1. Introduction

The self-assembly and directed assembly of patterned functional surfaces have facilitated the creation of complex, well-ordered structures that can interact or react with their environment for applications ranging from biosensors[1] and bioactive systems[2,3] to molecular electronics[4,5] and lithography.[6−11] In most cases, well-defined, functional structures require multiple fabrication steps, increasing the probability of contamination, molecular diffusion, and pattern dissolution.[12] These side effects significantly hinder the fabrication of functional surfaces, affecting not only the nanoscale-patterned features, but also the overall functionality of devices. These detrimental effects can be minimized by using labile layers to control deposition and to reduce surface contamination, if the layers can withstand other fabrication processes and are easily removable when desired.[13,14]

Previously, we have shown that 1-adamantanethiolate (AD) SAMs can be used to enhance existing microcontact printing techniques by providing a labile monolayer that undergoes complete molecular exchange in the contact areas while the remaining AD SAM domains in the uncontacted areas act as lateral diffusion barriers.[7] The labile nature of this monolayer results in sharper, higher quality features, while extending the library of patternable molecules to those that would not otherwise retain their patterned structures.[8] The AD SAMs not only control the deposition rate and minimize surface contamination, but also protect the integrity of the patterned features.[15] However, in order for AD SAMs to be widely used as molecular resists for chemical and soft lithography, they would need to withstand a variety of fabrication steps; unfortunately, the highly labile nature of the SAM, while necessary for the desired exchange to occur, results in a SAM that rapidly exchanges with virtually any alkanethiol or related molecule in contact with its surface.[16−18] This limits AD SAMs to patterning

(1) Huang, L.; Reekmans, G.; Saerens, D.; Friedt, J. M.; Frederix, F.; Francis, L.; Muyldermans, S.; Campitelli, A.; Van Hoof, C. *Biosens. Bioelectron.* **2005**, *21*, 483–490.
(2) Kwok, C. S.; Mourad, P. D.; Crum, L. A.; Ratner, B. D. *Biomacromolecules* **2000**, *1*, 139–148.
(3) Mullen, T. J.; Dameron, A. A.; Andrews, A. M.; Weiss, P. S. *Aldrichimica Acta* **2007**, *40*, 21–31.
(4) Mantooth, B. A.; Weiss, P. S. *Proc. IEEE* **2003**, *91*, 1785–1802.
(5) Moore, A. M.; Dameron, A. A.; Mantooth, B. A.; Smith, R. K.; Fuchs, D. J.; Ciszek, J. W.; Maya, F.; Yao, Y. X.; Tour, J. M.; Weiss, P. S. *J. Am. Chem. Soc.* **2006**, *128*, 1959–1967.
(6) Anderson, M. E.; Mihok, M.; Tanaka, H.; Tan, L. P.; Horn, M. W.; McCarty, G. S.; Weiss, P. S. *Adv. Mater.* **2006**, *18*, 1020–1022.
(7) Dameron, A. A.; Hampton, J. R.; Smith, R. K.; Mullen, T. J.; Gillmor, S. D.; Weiss, P. S. *Nano Lett.* **2005**, *5*, 1834–1837.
(8) Dameron, A. A.; Hampton, J. R.; Gillmor, S. D.; Hohman, J. N.; Weiss, P. S. *J. Vac. Sci. Technol., B* **2005**, *23*, 2929–2932.
(9) Smith, R. K.; Lewis, P. A.; Weiss, P. S. *Prog. Surf. Sci.* **2004**, *75*, 1–68.
(10) Mullen, T. J.; Srinivasan, C.; Hohman, J. N.; Gillmor, S. D.; Shuster, M. J.; Horn, M. W.; Andrews, A. M.; Weiss, P. S. *Appl. Phys. Lett.* **2007**, *90*, 063114.
(11) Weiss, P. S. *Acc. Chem. Res.* **2008**, *41*, 1772–1781.
(12) Delamarche, E.; Schmid, H.; Bietsch, A.; Larsen, N. B.; Rothuizen, H.; Michel, B.; Biebuyck, H. *J. Phys. Chem. B* **1998**, *102*, 3324–3334.
(13) Tanaka, H.; Anderson, M. E.; Horn, M. W.; Weiss, P. S. *Jpn. J. Appl. Phys., Part 2* **2004**, *43*, L950–L953.
(14) Anderson, M. E.; Srinivasan, C.; Hohman, J. N.; Carter, E. M.; Horn, M. W.; Weiss, P. S. *Adv. Mater.* **2006**, *18*, 3258–3260.
(15) Madueno, R.; Raisanen, M. T.; Silien, C.; Buck, M. *Nature* **2008**, *454*, 618–621.
(16) Dameron, A. A.; Mullen, T. J.; Hengstebeck, R. W.; Saavedra, H. M.; Weiss, P. S. *J. Phys. Chem. C* **2007**, *111*, 6747–6752.
(17) Mullen, T. J.; Dameron, A. A.; Saavedra, H. M.; Williams, M. E.; Weiss, P. S. *J. Phys. Chem. C* **2007**, *111*, 6740–6746.

10.1021/ja807648g CCC: $40.75

strategies that expose thiols only to the specific areas of the SAM that would result in the desired pattern while preventing subsequent fabrication steps.

In order to obtain more precise control over a single functionality, molecule, or patterned feature on a surface, a methodology similar to resist exposure in photolithography needs to be developed to make robust SAMs that are resistant to molecular exchange, and undergo rapid and switchable displacement when desired. Previous studies have shown that molecular exchange in well-ordered SAMs other than AD undergo an inhomogeneous process, where rapid exchange (minutes to hours) occurs at grain boundaries, defects, and other disordered regions while occurring slowly in the crystalline domains, taking from days to weeks to reach steady state, but often incomplete, displacement (30−60%).[19−22] Therefore, in order to achieve more homogeneous and controlled displacement over a selected region of a SAM, the degree of order in these crystalline regions needs to be tuned after the self-assembly process but prior to the desired fabrication step.

Previously, Bumm et al. applied thermal processing to modify SAMs after their self-assembly.[3,23] By heating an alkanethiolate SAM in the presence of excess thiol in solution, the densities of structural domain boundaries and Au substrate vacancy islands were decreased dramatically. The elevated temperatures led to Ostwald ripening of the SAM domains, assisted by an increase in surface diffusion and by acceleration in alkanethiolate desorption/adsorption.[24−30] In this way, the crystalline domain sizes were limited by the terrace size of the underlying Au substrate. Along these lines, Cyganic et al. annealed 2-(aryl)ethane thiolate SAMs under a nitrogen atmosphere, leading to a phase transition that dramatically improved the film stability (demonstrated by exchange experiments).[31]

However, in order to fabricate complex chemical patterns, a complementary approach is required, in which SAMs are purposefully disrupted to enable molecular exchange. To this end, ultraviolet (UV) and low-energy electron irradiation have been used to create chemical and structural defects in alkanethiolate SAMs to promote molecular exchange.[13,14,32−36] Using such techniques, Ballav et al. successfully increased exchange rates by an order of magnitude while tuning the degree of exchange from 10% to 100%. However, this type of irradiation irreversibly damages the exposed regions, whether via oxidation of the thiol headgroup or by dehydrogenation of the SAM. It is thus limited to the resolution and capabilities of top-down lithographic approaches and does not take full advantage of the chemical nature of the film. Exploiting the chemistry of the molecules enables the independent manipulation of a single functionality in the film, thereby allowing precise patterning and/or modification of molecules while tailoring the surface reactivity of the resulting film at the supramolecular 1−100 nm scale without the need for expensive nanofabrication facilities.[37−39] Here, we employ a simple chemical reaction, Fischer esterification, to create subtle chemical and structural defects in carboxylic-acid-terminated SAMs, thereby promoting the partial or complete molecular exchange of a robust, well-ordered SAM. We also utilize the complementary hydrolysis reaction to regain the carboxylic acid termini, thus quenching further molecular exchange, as illustrated in Scheme 1. These chemical and structural changes were measured with infrared reflection absorption spectroscopy (IRRAS) and X-ray photoelectron spectroscopy (XPS), to monitor the properties and composition of the resulting film, demonstrating that well-ordered and otherwise stable monolayers can be controllably exchanged with molecules in solution using these step-by-step reactions.

Scheme 1. Reaction and Patterning Scheme of the Chemically Induced Exchange Reactions in 11-Mercaptoundecanoic Acid (MUDA) SAMs[a]

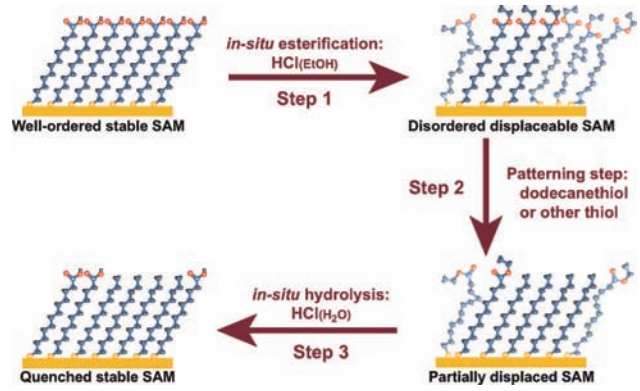

[a] Exposure to HCl and ethanol leads to the formation of a disordered ester intermediate, 1-ethyl-11-mercaptoundecanoate (*in situ* esterified MUDA). Subsequent exposure to *n*-dodecanethiol (C12) solution allows tunable (fractional or complete) displacement of the reactive intermediate. Sections of the SAM containing undisplaced ethyl ester molecules can be hydrolyzed and quenched to prevent further exchange or displacement by exposure to aqueous HCl. The same patterning scheme was also applied to 3-mercapto-1-adamantanecarboxylic acid (MADCA) SAMs.

2. Experimental Methods

2.1. Monolayer Preparation. Gold substrates, 1000 Å thick (99.999%, Kurt J. Lesker, Clairton, PA), were prepared with an electron-beam evaporator using 4 in. polished silicon ⟨100⟩ wafers (Silicon Quest Int., Santa Clara, CA) with a 100 Å chromium

(18) Saavedra, H. M.; Barbu, C. M.; Dameron, A. A.; Mullen, T. J.; Crespi, V. H.; Weiss, P. S. *J. Am. Chem. Soc.* **2007**, *129*, 10741–10746.
(19) Kassam, A.; Bremner, G.; Clark, B.; Ulibarri, G.; Lennox, R. B. *J. Am. Chem. Soc.* **2006**, *128*, 3476–3477.
(20) Lussem, B.; Muller-Meskamp, L.; Karthauser, S.; Waser, R.; Homberger, M.; Simon, U. *Langmuir* **2006**, *22*, 3021–3027.
(21) Kolega, R. R.; Schlenoff, J. B. *Langmuir* **1998**, *14*, 5469–5478.
(22) Schlenoff, J. B.; Li, M.; Ly, H. *J. Am. Chem. Soc.* **1995**, *117*, 12528–12536.
(23) Bumm, L. A.; Arnold, J. J.; Charles, L. F.; Dunbar, T. D.; Allara, D. L.; Weiss, P. S. *J. Am. Chem. Soc.* **1999**, *121*, 8017–8021.
(24) Schreiber, F.; Eberhardt, A.; Leung, T. Y. B.; Schwartz, P.; Wetterer, S. M.; Lavrich, D. J.; Berman, L.; Fenter, P.; Eisenberger, P.; Scoles, G. *Phys. Rev. B* **1998**, *57*, 12476–12481.
(25) Schonenberger, C.; Jorritsma, J.; Sondaghuethorst, J. A. M.; Fokkink, L. G. J. *J. Phys. Chem.* **1995**, *99*, 3259–3271.
(26) Delamarche, E.; Michel, B.; Kang, H.; Gerber, C. *Langmuir* **1994**, *10*, 4103–4108.
(27) McCarley, R. L.; Dunaway, D. J.; Willicut, R. J. *Langmuir* **1993**, *9*, 2775–2777.
(28) Bucher, J. P.; Santesson, L.; Kern, K. *Langmuir* **1994**, *10*, 979–983.
(29) Delamarche, E.; Michel, B. *Thin Solid Films* **1996**, *273*, 54–60.
(30) Dubois, L. H.; Nuzzo, R. G. *Annu. Rev. Phys. Chem.* **1992**, *43*, 437–463.
(31) Cyganik, P.; Buck, M.; Strunskus, T.; Shaporenko, A.; Witte, G.; Zharnikov, M.; Wöll, C. *J. Phys. Chem. C* **2007**, *111*, 16909–16919.
(32) Ballav, N.; Shaporenko, A.; Krakert, S.; Terfort, A.; Zharnikov, M. *J. Phys. Chem. C* **2007**, *111*, 7772–7782.
(33) Ballav, N.; Weidner, T.; Zharnikov, M. *J. Phys. Chem. C* **2007**, *111*, 12002–12010.
(34) Ballav, N.; Shaporenko, A.; Terfort, A.; Zharnikov, M. *Adv. Mater.* **2007**, *19*, 998–1000.
(35) Ballav, N.; Weidner, T.; Rossler, K.; Lang, H.; Zharnikov, M. *ChemPhysChem* **2007**, *8*, 819–822.
(36) Zharnikov, M.; Shaporenko, A.; Paul, A.; Golzhauser, A.; Scholl, A. *J. Phys. Chem. B* **2005**, *109*, 5168–5174.
(37) Mullen, T. J.; Srinivasan, C.; Shuster, M. J.; Horn, M. W.; Andrews, A. M.; Weiss, P. S. *J. Nanopart. Res.* **2008**, *10*, 1231–1240.

Scheme 2

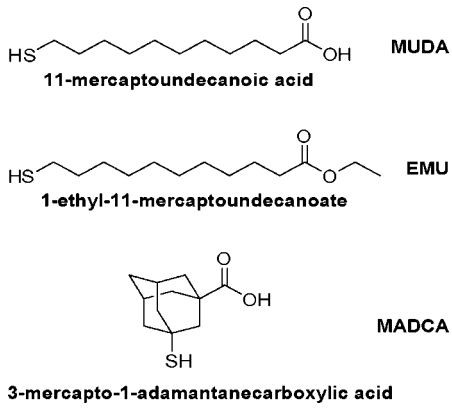

adhesion layer (99.998%, Kurt J. Lesker, Clairton, PA). Monolayers were fabricated by immersing freshly prepared, hydrogen-flame-annealed gold substrates into ethanolic solutions of the desired thiol molecule. *n*-Dodecanethiolate (C12), perdeuterated *n*-dodecanethiolate ($C12_{d25}$), and 1-ethyl-11-mercaptoundecanoate[40] (EMU) SAMs were prepared from 1.0 mM solutions, while 11-mercaptoundecanoic acid (MUDA) (Sigma-Aldrich, St. Louis, MO) and 3-mercapto-1-adamantanecarboxylic acid (MADCA) (Matrix Scientific, Columbia, SC) SAMs were prepared from 1.0 mM solutions containing 10% acetic acid (Scheme 2).[41,42] After deposition for 24 h, the gold substrates were removed, rinsed with ethanol, and dried under a stream of nitrogen. All SAMs were used immediately after preparation.

2.2. Infrared Reflection Absorption Spectroscopy. Infrared absorption spectra were collected using a Nicolet 6700 FTIR spectrometer (Thermo Electron Corp., Madison, WI) equipped with a liquid-nitrogen-cooled mercury−cadmium−telluride detector and a Seagull variable-angle reflection accessory (Harrick Scientific Inc., Ossining, NY). The spectrometer was purged with dry and CO_2-free air produced by an FTIR purge gas generator (Parker-Balston, Cleveland, OH). The spectra were collected at grazing incidence reflection (84° relative to the surface normal) with *p*-polarized light and a mirror speed of 1.27 cm/s, with a resolution of 2 cm^{-1}. Spectra were transformed using Norton−Beer (N−B) medium apodization, averaged over 1024 scans, and normalized with data recorded from $C12_{d25}$ SAMs.

2.3. X-ray Photoelectron Spectroscopy. X-ray photoelectron spectra were acquired using a Kratos Axis Ultra spectrometer (Chestnut Ridge, NY) with a monochromatic Al Kα source (20 mA, 1.4 keV), a base pressure of 1×10^{-9} Torr, and a spot size of 300 μm × 700 μm. Survey spectra were acquired at a pass energy of 80 eV, while high-resolution spectra of the O 1s, C 1s, S 2p, and Au 4f regions were collected at a pass energy of 20 eV. The binding energies (E_b's) were referenced to the Au $4f_{7/2}$ peak at 83.98 eV. All of the peaks from the spectra were fit using Gaussian−Lorentzian (GL) line shapes using a Shirley-type background. The Au 4f peaks were fit with a fixed energy separation of 3.68 eV and a fixed-area ratio of 3:4. The S $2p_{3/2,1/2}$ doublet peaks were fit using a fixed-energy separation of 1.18 eV, and a fixed-area ratio of 1:2.

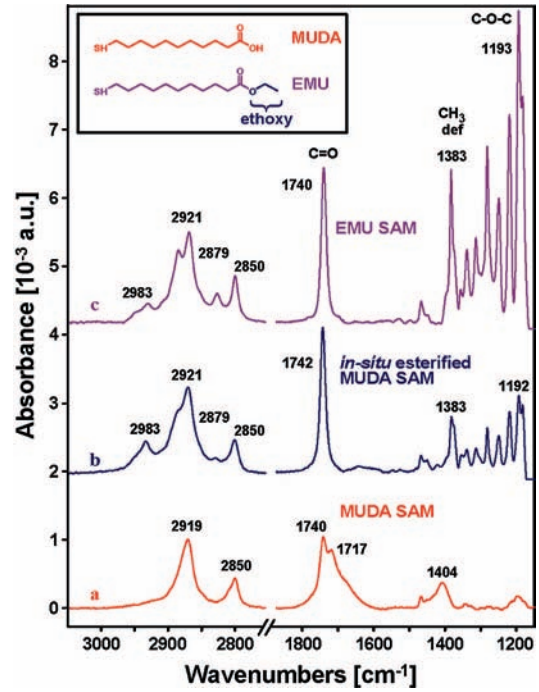

Figure 1. Representative IRRAS spectra of a 11-mercaptoundecanoic acid (MUDA) SAM (a) before and (b) after *in situ* esterification, which consists of 24-h exposure to ethanolic 0.6 M HCl. The spectrum after Fischer esterification shows the characteristic absorptions of an ester. (c) Spectrum of a 1-ethyl-11-mercaptoundecanoate (EMU) SAM deposited from 1.0 mM EMU solution. The inset shows the structure of MUDA and EMU molecules.

3. Results and Discussion

3.1. Characterization of 11-Mercaptoundecanoic Acid, *in Situ* Esterified 11-Mercaptoundecanoic Acid, and 1-Ethyl-11-Mercaptoundecanoate SAMs (Step 1, Scheme 1). We use IRRAS and XPS to provide detailed, quantitative information on film structure and composition. Grazing incidence IRRAS spectra of SAMs were obtained from 800 to 4000 cm^{-1}. Figure 1a (red) shows a typical spectrum of a pristine MUDA SAM. The 2800−3100 cm^{-1} region in the MUDA SAM spectrum is dominated by the characteristic stretching bands of methylene groups, in which the positions of the symmetric and asymmetric stretching modes are located at ∼2850 and ∼2920 cm^{-1}, respectively.[43−48] These are in agreement with the literature values of 2850 and 2919 cm^{-1}, which are indicative of crystalline-like packing of the alkyl chains.[49−51] These features suggest a predominantly all-*trans* configuration of the alkyl chains, with few gauche defects. The broad 1740 and 1404 cm^{-1} absorption bands in the 1100 to 1800 cm^{-1} region correspond to the carboxyl and carboxylate C═O stretches. The broad carboxyl C═O absorption can be attributed

(38) Geyer, W.; Stadler, V.; Eck, W.; Zharnikov, M.; Golzhauser, A.; Grunze, M. *Appl. Phys. Lett.* **1999**, *75*, 2401–2403.
(39) Golzhauser, A.; Eck, W.; Geyer, W.; Stadler, V.; Weimann, T.; Hinze, P.; Grunze, M. *Adv. Mater.* **2001**, *13*, 806–809.
(40) Bader, M. M. *Phosphorus, Sulfur Silicon Relat. Elem.* **1996**, *116*, 77–92.
(41) Arnold, R.; Azzam, W.; Terfort, A.; Wöll, C. *Langmuir* **2002**, *18*, 3980–3992.
(42) Himmel, H. J.; Terfort, A.; Wöll, C. *J. Am. Chem. Soc.* **1998**, *120*, 12069–12074.
(43) Nuzzo, R. G.; Allara, D. L. *J. Am. Chem. Soc.* **1983**, *105*, 4481–4483.
(44) Allara, D. L.; Nuzzo, R. G. *Langmuir* **1985**, *1*, 52–66.
(45) Allara, D. L.; Nuzzo, R. G. *Langmuir* **1985**, *1*, 45–52.
(46) Nuzzo, R. G.; Dubois, L. H.; Allara, D. L. *J. Am. Chem. Soc.* **1990**, *112*, 558–569.
(47) Laibinis, P. E.; Whitesides, G. M.; Allara, D. L.; Tao, Y. T.; Parikh, A. N.; Nuzzo, R. G. *J. Am. Chem. Soc.* **1991**, *113*, 7152–7167.
(48) Atre, S. V.; Liedberg, B.; Allara, D. L. *Langmuir* **1995**, *11*, 3882–3893.
(49) Muller, H. U.; Zharnikov, M.; Volkel, B.; Schertel, A.; Harder, P.; Grunze, M. *J. Phys. Chem. B* **1998**, *102*, 7949–7959.
(50) Yan, C.; Golzhauser, A.; Grunze, M.; Wöll, C. *Langmuir* **1999**, *15*, 2414–2419.
(51) Zharnikov, M.; Grunze, M. *J. Vac. Sci. Technol., B* **2002**, *20*, 1793–1807.

to the free and hydrogen-bonded forms observed in MUDA SAMs, which occur between 1700 and 1740 cm^{-1}.[41]

The spectrum of the MUDA SAM (Figure 1a, red) after 24 h exposure to 0.62 M ethanolic HCl solution (*in situ* esterified MUDA, Figure 1b, green) shows a shift in the asymmetric methylene absorption band (2921 cm^{-1}), indicating lower conformational and orientational order in the SAM. The position of this absorption is highly sensitive to the conformational order of the alkyl chains and varied among samples from 2921 to 2923 cm^{-1}, in which the upper value is characteristic of liquid-like disorder.[52−55] Additional bands in the aliphatic C−H stretch region were also observed. These bands, 2879 and 2983 cm^{-1}, are characteristic of methyl symmetric and asymmetric stretching modes. Variations are also observed in the carbonyl stretching absorption, which becomes considerably sharper and stronger while shifting to 1742 cm^{-1}, characteristic of a predominantly non-hydrogen-bonded carbonyl stretch.[41] However, the largest variations are observed in the 1100−1400 cm^{-1} region, where multiple sharp and well-defined absorption bands are now present. These bands have been observed previously, and are characteristic of alkyl esters.[41] The 1383 and 1192 cm^{-1} absorption bands correspond to a C−O stretch and a methyl rocking mode, respectively.

The C 1s XPS spectra of a pristine MUDA SAM and an *in situ* esterified MUDA SAM are shown in Figure 2. For the MUDA SAM (Figure 2a), the C 1s emission can be fit to two GL lineshapes: a low intensity peak centered at 289.5 eV and a much higher intensity peak centered at 284.8 eV. The more intense, lower-energy peak is attributed to the hydrocarbon backbone of the MUDA molecules, while the low intensity peak is attributed to the carbonyl carbon. Both of these features are in agreement with literature values.[46,47,56,57] The MUDA aliphatic chain XPS C 1s emission with $E_b = 284.8$ eV is in agreement with the literature values for *n*-dodecanethiolate SAMs ($E_b = 284.9$ eV), indicating a densely packed and contamination-free SAM. The S 2p XPS spectrum (data not shown) exhibits a single S $2p_{3/2,1/2}$ doublet ($E_b = 162.1$, 163.2 eV), corresponding to the Au−thiolate bond.

The XPS C 1s spectrum of the MUDA SAM changed upon *in situ* esterification (Figure 2b). The C 1s aliphatic chain emission shifted to a lower energy (284.1 eV) and slightly decreased in intensity (5 ± 1%) with respect to that of the MUDA SAM. The slight decrease in intensity indicates partial desorption of the initial MUDA SAM, while the peak shift reflects structural and/or chemical changes in the film consistent with the disorder observed with IRRAS. The aliphatic chain peak was also found to be asymmetric, with a wider tail and a shoulder on the high E_b side. The C 1s spectrum was therefore fit with four GL line shapes. The two additional features, centered at 286.4 and 285.2 eV, have an area ratio of approximately 1:1. These features have been previously observed in XPS spectra of alkyl esters, and were attributed to the carbon backbone of the alkoxy portion of the molecule.[58] The higher energy peak corresponds to the carbon

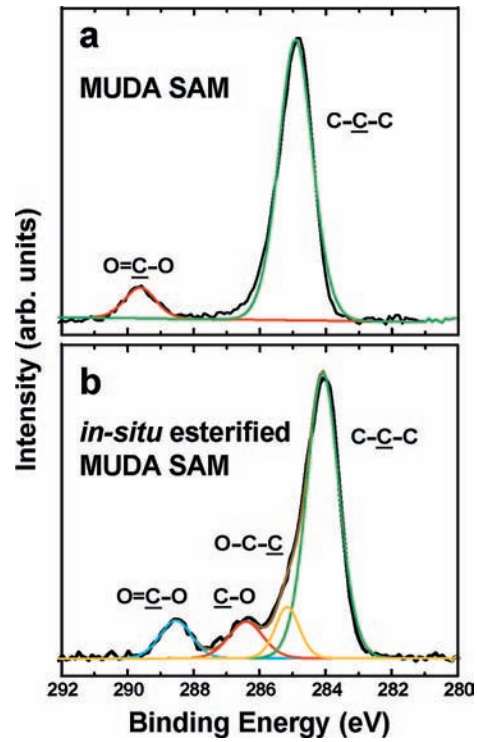

Figure 2. X-ray photoelectron spectra of the C 1s region of MUDA SAMs (a) before and (b) after *in situ* esterification. Each spectrum was fit with Gaussian−Lorentzian line shapes, revealing contributions from the carbonyl carbon (blue), the ethoxy methylene (red), the methyl of the ethoxy (yellow), and the alkyl methylenes (green). The C 1s spectrum of the Fischer esterification product reveals characteristic peaks of ethyl esters, and the resulting 1:1:1 area ratio between the carbonyl carbon, ethoxy methylene, and the terminal methyl of the ethoxy indicates that the reaction proceeds to near completion.

bonded to the ester functionality, while the lower-energy emission corresponds to the rest of the carbon backbone in the alkoxy group. It is important to note that neither shifts nor broadening of the Au $4f_{7/2}$ emissions were observed, which would have indicated the presence of gold oxide.[50,59−61]

Both IRRAS and XPS spectra show the appearance of methyl groups in the *in situ* esterified MUDA SAM, indicating a chemical and structural change in the film. Further evidence is provided by the sharp carbonyl stretch, which is no longer broadened by hydrogen bonding. However, the appearance of the multiple bands in the 1100−1400 cm^{-1} region of the IRRAS spectrum sheds light onto the chemical identity of the resulting SAM, specifically the 1192 cm^{-1} band of the C−O stretch, which suggests the formation of an ester. Ethanol is the only alcohol present for reaction via Fischer esterification, which indicates the formation of an ethyl ester. Furthermore, direct evidence of ethyl ester formation is observed in the XPS spectra, which shows a 1:1 area ratio between the two features corresponding to the alkoxy portion of the ester. This ratio relates the carbon bonded to the ester functionality and the remaining carbons of the alkoxy backbone. The 1:1 area relationship indicates an alkoxy backbone that is only two carbons long, which suggests the formation of 1-ethyl-11-mercaptoundecanoate. Furthermore, the spectrum also shows a 1:1 area relationship between the carbonyl carbon emission and the emission from

(52) Bensebaa, F.; Ellis, T. H.; Badia, A.; Lennox, R. B. *Langmuir* **1998**, *14*, 2361–2367.
(53) Bensebaa, F.; Ellis, T. H.; Badia, A.; Lennox, R. B. *J. Vac. Sci. Technol., A* **1995**, *13*, 1331–1336.
(54) Porter, M. D.; Bright, T. B.; Allara, D. L.; Chidsey, C. E. D. *J. Am. Chem. Soc.* **1987**, *109*, 3559–3568.
(55) Whitesides, G. M.; Laibinis, P. E. *Langmuir* **1990**, *6*, 87–96.
(56) Duwez, A. S. *J. Electron Spectrosc. Relat. Phenom.* **2004**, *134*, 97–138.
(57) Laibinis, P. E.; Bain, C. D.; Whitesides, G. M. *J. Phys. Chem.* **1991**, *95*, 7017–7021.
(58) Moulder, J. F.; Stickle, W. F.; Sobol, P. E.; Bomben, K. D. *Handbook of X-Ray Photoelectron Spectroscopy*; Perkin-Elmer: Eden Prairie, MN, 1992.
(59) Pireaux, J. J.; Chtaib, M.; Delrue, J. P.; Thiry, P. A.; Liehr, M.; Caudano, R. *Surf. Sci.* **1984**, *141*, 211–220.
(60) Pireaux, J. J.; Liehr, M.; Thiry, P. A.; Delrue, J. P.; Caudano, R. *Surf. Sci.* **1984**, *141*, 221–232.
(61) Ron, H.; Rubinstein, I. *Langmuir* **1994**, *10*, 4566–4573.

the carbon closest to the ester functionality on the alkoxy portion of the ester. This indicates that the film is completely esterified, since in a partially esterified film the ratio would favor the carbonyl carbon.

To complement the characterization of the products resulting from the *in situ* esterification, the corresponding ester thiol, 1-ethyl-11-mercaptoundecanoate (EMU), was synthesized and purified in order to investigate pristine and unreacted EMU SAMs. Figure 1c shows a representative IRRAS spectrum of an EMU SAM deposited from a 1.0 mM EMU solution, which exhibits similarities to spectra of *in situ* esterified MUDA SAMs. The absorptions occur at the same positions, although there are variations in peak intensities. In the 2800−3100 cm^{-1} region of the EMU SAM spectrum, the asymmetric methyl stretch absorption (2983 cm^{-1}) is considerably weaker and barely visible, while the symmetric methyl stretch absorption (2879 cm^{-1}) is stronger and better defined, when compared to those of *in situ* esterified MUDA SAMs. However, the largest variations in the EMU SAM spectrum are observed in the 1100−1400 cm^{-1} region, where the multiple absorption bands characteristic of esters are roughly twice as intense, as compared to the *in situ* esterified MUDA SAM spectrum. These intensity differences, which are due to the surface selection rules of IRRAS, indicate differences in the packing and in the conformational order of the terminal chains, which are the reacted portions of the molecules in the *in situ* esterified SAM.[62−64] It is assumed that the EMU SAM deposited from solution has greater conformational order at the tail termini, since packing is better optimized during the self-assembly process.

3.2. Displacement of 11-Mercaptoundecanoic Acid, *in Situ* Esterified 11-Mercaptoundecanoic Acid, 1-Ethyl-11-mercaptoundecanoate, and *n*-Dodecanethiolate SAMs (Step 2, Scheme 1). Previous work has shown that molecules with stronger intermolecular interactions can exchange into SAMs, displacing adsorbates that interact more weakly.[65−69] It is important to note that currently only a handful of monolayers, such as AD with its tailored intermolecular interactions and lower packing density, form labile layers that readily and completely exchange with other thiols. For other SAMs, only partial exchange is typically achieved, reaching a fractional value even after several days of thiol exposure.[19−22] Figure 3a,b shows representative IRRAS spectra of MUDA SAMs before and after 1 h exposure to a 1.0 mM C12 solution. After exposure, the SAM showed symmetric and asymmetric methyl stretch absorptions. Due to the chemical composition of the unreacted MUDA SAM, only bands corresponding to the methylene stretches should be observed, in the absence of exchange with C12 molecules. The appearance of both methyl bands, and subsequent increases in intensity with further exposure, suggests molecular insertion and exchange of the MUDA SAM with the C12 solution.[18] The low intensity of the methyl absorptions, and thus the limited extent

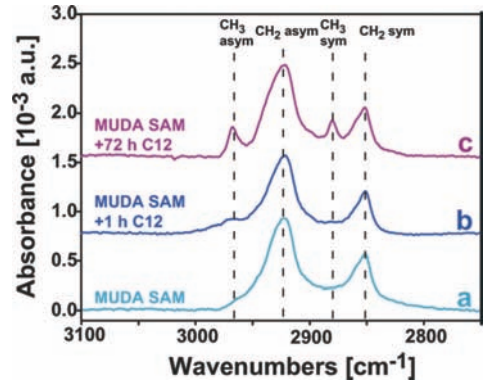

Figure 3. (a) Representative IRRAS spectra of an 11-mercaptoundecanoic acid (MUDA) SAM before displacement, and the resulting spectra after (b) 1 h and (c) 72 h exposure to 1.0 mM *n*-dodecanethiol (C12) solution. These spectra indicate that limited displacement is observed in untreated MUDA SAMs.

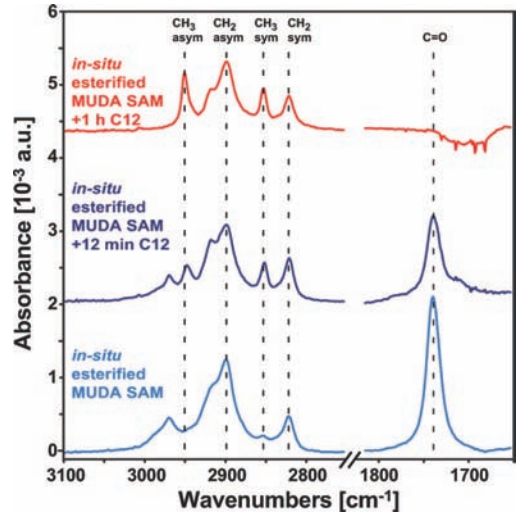

Figure 4. (a) Representative IRRAS spectra of an *in situ* esterified 11-mercaptoundecanoic acid (MUDA) SAM before displacement, and the resulting spectra after (b) 12 min and (c) 1 h exposures to 1.0 mM *n*-dodecanethiol (C12) solution. The disappearance of the carbonyl stretch after 1 h exposure indicates the lack of MUDA molecules, showing that *in situ* esterification promotes complete molecular exchange.

of molecular exchange, indicates a high-quality and densely packed SAM that is not particularly susceptible to displacement.[70] A higher degree of molecular exchange was achieved after 71 h exposure to 1.0 mM C12 solution (Figure 3c), resulting in spectra with contributions from both molecules, with peaks at 2879 and 2966 cm^{-1}. However, the integrated areas of these peaks relative to those of a pristine C12 SAM reveal that only 29 ± 4% of the MUDA SAM was exchanged, in agreement with literature values.[10]

Greater impact on molecular exchange kinetics can be achieved by treating the MUDA SAM with an ethanolic HCl solution, leading to the formation of the corresponding ethyl ester. Figure 4 shows representative IRRAS spectra of an *in situ* esterified MUDA SAM before and after 12 min and 1 h exposures to 1.0 mM C12 solution. The 1 h spectrum has sharp and well-defined absorption peaks at 2878 and 2985 cm^{-1}, as well as a shoulder at 2937 cm^{-1}, corresponding to the C12 methyl stretch modes. Furthermore, the full-width-at-half-

(62) Terrill, R. H.; Tanzer, T. A.; Bohn, P. W. *Langmuir* **1998**, *14*, 845–854.
(63) Tamada, K.; Nagasawa, J.; Nakanishi, F.; Abe, K.; Ishida, T.; Hara, M.; Knoll, W. *Langmuir* **1998**, *14*, 3264–3271.
(64) Parikh, A. N.; Allara, D. L. *J. Chem. Phys.* **1992**, *96*, 927–945.
(65) Chidsey, C. E. D.; Bertozzi, C. R.; Putvinski, T. M.; Mujsce, A. M. *J. Am. Chem. Soc.* **1990**, *112*, 4301–4306.
(66) Folkers, J. P.; Laibinis, P. E.; Whitesides, G. M.; Deutch, J. *J. Phys. Chem.* **1994**, *98*, 563–571.
(67) Collard, D. M.; Fox, M. A. *Langmuir* **1991**, *7*, 1192–1197.
(68) Biebuyck, H. A.; Bian, C. D.; Whitesides, G. M. *Langmuir* **1994**, *10*, 1825–1831.
(69) Patole, S. N.; Baddeley, C. J.; O'Hagan, D.; Richardson, N. V. *J. Phys. Chem. C* **2008**, *112*, 13997–14000.
(70) Love, J. C.; Estroff, L. A.; Kriebel, J. K.; Nuzzo, R. G.; Whitesides, G. M. *Chem. Rev.* **2005**, *105*, 1103–1169.

maximum (fwhm) of the asymmetric methylene peak narrowed from 25 to 17 cm^{-1}, while shifting from 2921 to 2919 cm^{-1}, indicating the presence of a well-ordered alkanethiolate SAM in a predominantly all-*trans* configuration, also supported by the disappearance of the carbonyl stretch at 1742 cm^{-1}. The spectrum was therefore nearly identical to the spectrum of a single-component C12 SAM fabricated on a bare gold substrate, indicating that the fractional *in situ* esterified MUDA coverage has been significantly diminished. It is important to note that although the resulting spectrum is almost identical to that of a pristine C12 SAM, slight variations are evident even after 24 h exposure to the displacing solution (data not shown). For example, the integrated area and intensity of the methyl stretch modes were somewhat smaller than those of a pristine C12 SAM, indicating lower molecular density in the resultant SAM. Furthermore, the intensity ratios between all the methyl and methylene stretch modes were slightly different, and indicated a larger number of defects in the resultant SAM.[38,44−51,71] These IRRAS spectral differences have been previously observed in C12 SAMs formed by the displacement of pre-existing AD SAMs.[17] In that study, scanning tunneling microscopy images of the resulting C12 SAM revealed smaller-sized domains and, thus, increased numbers of boundaries and defects. Mullen et al. attributed these differences in domain size to the nucleation-induced displacement of AD molecules, which kinetically traps molecular domains to their specific tilts, since they lack sufficient thermal energy to change the orientations of entire domains to match the orientations of neighboring molecules.

The exchange reaction is likely promoted by the formation of defects and disorder in the SAM that result from *in situ* esterification, as described above in the characterization of the *in situ* esterified SAMs. We suppose that this disorder is a consequence of the steric hindrance of the new terminal functionalities, which may be augmented by the reaction exothermicity.[9,23] Similar effects were observed by Mirkin and co-workers; in their experiments electrochemical reactions on inserted azobenzene moieties led to the disruption of the surrounding SAM.[72,73]

The degree of molecular exchange in EMU SAMs was also determined, as described below. Figure 5 shows the IRRAS spectra of an EMU SAM deposited from a 1.0 mM EMU solution before and after 1 h exposure to 1.0 mM C12 solution. The symmetric and asymmetric methyl absorptions at 2960 and 2877 cm^{-1}, respectively, slightly increased in intensity (13 ± 1%), while the carbonyl and ester bands decreased slightly in intensity (9 ± 1%). This indicates a limited degree of molecular exchange, since increases in the methyl absorptions are mostly due to molecular insertion at defect sites, as previously observed in alkanethiolate SAMs.[3,4,9,10,74−78] Therefore, the stability of the EMU SAM, and its ability to undergo molecular exchange, is similar to alkanethiolate SAMs. The stability differences between the EMU and *in situ* esterified MUDA SAMs can be explained by their spectral differences, which indicate greater disorder in the latter SAM, as described above.

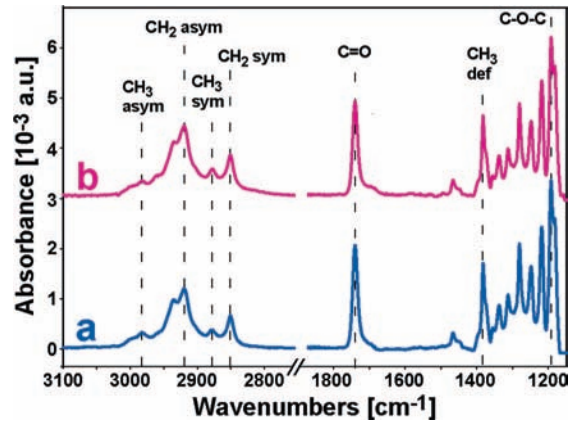

Figure 5. (a) Representative IRRAS spectrum of 1-ethyl-11-mercaptoundecanoate (EMU) SAM formed from 1.0 mM EMU solution. (b) The resulting spectrum after 1 h exposure to 1.0 mM *n*-dodecanethiol (C12) solution. Small intensity changes, such as the decrease in the carbonyl group absorption and the increase in the symmetric methyl mode absorption, indicate small amounts of molecular exchange even though the SAM is chemically identical at the molecular level of each molecule to the *in situ* esterified MUDA SAM. This suggests that differences in the degree of disorder, and in the assembly, play important roles.

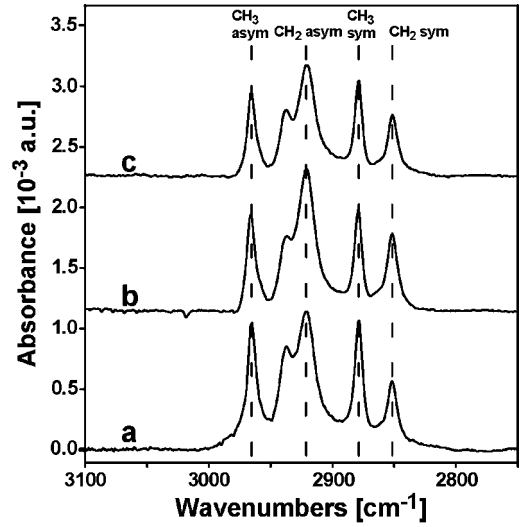

Figure 6. Representative IRRAS spectra of an *n*-dodecanethiolate (C12) SAM (a) before displacement, (b) after exposure to similar Fischer esterification conditions used to esterify MUDA SAMs, and (c) after 1 h exposure to 1.0 mM perdeuterated *n*-dodecanethiol ($C12_{d25}$) solution. The minor spectral changes after exposure to the C12 solution demonstrate that robust unfunctionalized SAMs can withstand the *in situ* esterification without leading to significant molecular exchange with further thiol exposure.

To create a complex chemically patterned surface, it will be necessary to react specific molecules or patterns in a SAM selectively without disturbing the surrounding matrix. In order to determine the stability of an unfunctionalized SAM that could serve as a surrounding matrix, a pristine C12 SAM was exposed to *in situ* esterification conditions. Figure 6a shows the IRRAS spectrum of a pristine C12 SAM, which is dominated by the characteristic stretching bands of methyl and methylene groups (*vide supra*). The position of the asymmetric methylene stretch was found to be 2919 cm^{-1}, which is again in agreement with literature values for crystalline-like films with predominantly all-*trans* configurations.

(71) Tao, Y. T.; Lin, W. L.; Hietpas, G. D.; Allara, D. L. *J. Phys. Chem. B* **1997**, *101*, 9732–9740.
(72) Caldwell, W. B.; Campbell, D. J.; Chen, K. M.; Herr, B. R.; Mirkin, C. A.; Malik, A.; Durbin, M. K.; Dutta, P.; Huang, K. G. *J. Am. Chem. Soc.* **1995**, *117*, 6071–6082.
(73) Walter, D. G.; Campbell, D. J.; Mirkin, C. A. *J. Phys. Chem. B* **1999**, *103*, 402–405.
(74) Stranick, S. J.; Parikh, A. N.; Tao, Y. T.; Allara, D. L.; Weiss, P. S. *J. Phys. Chem.* **1994**, *98*, 7636–7646.
(75) Cygan, M. T.; Dunbar, T. D.; Arnold, J. J.; Bumm, L. A.; Shedlock, N. F.; Burgin, T. P.; Jones, L.; Allara, D. L.; Tour, J. M.; Weiss, P. S. *J. Am. Chem. Soc.* **1998**, *120*, 2721–2732.
(76) Dunbar, T. D.; Cygan, M. T.; Bumm, L. A.; McCarty, G. S.; Burgin, T. P.; Reinerth, W. A.; Jones, L.; Jackiw, J. J.; Tour, J. M.; Weiss, P. S.; Allara, D. L. *J. Phys. Chem. B* **2000**, *104*, 4880–4893.
(77) Lewis, P. A.; Donhauser, Z. J.; Mantooth, B. A.; Smith, R. K.; Bumm, L. A.; Kelly, K. F.; Weiss, P. S. *Nanotechnology* **2001**, *12*, 231–237.
(78) Fuchs, D. J.; Weiss, P. S. *Nanotechnology* **2007**, *18*, 044021.

This absorption is also sharper, with a fwhm of 16 cm^{-1}, as compared to the 26 cm^{-1} fwhm of the pristine MUDA SAM, reflecting higher conformational and orientational order, in agreement with previous experiments.[79] After exposing the SAMs to the *in situ* esterification reaction for 24 h, only minor changes in the spectra were observed (Figure 6b). The symmetric and asymmetric methyl absorptions at 2967 and 2877 cm^{-1}, respectively, decreased in intensity (19 ± 2%). Similar results, but smaller effects (8 ± 3%), were observed when a pristine C12 SAM was exposed to neat ethanol for 24 h (results not shown). This indicates slight degradation, *not* due to reaction, of the C12 SAM when exposed to neat ethanol, in agreement with previous experiments showing that alkanethiolate SAMs can desorb to some extent as disulfides.[80−83] The rate and extent of desorption are highly dependent on the solvent; even small changes in the solvent composition (e.g., the addition of 5% dimethylformamide to water) can affect desorption.[80] Thus, it is not surprising that the extent of desorption into the acid/ethanol mixture is somewhat different than that for neat ethanol. Therefore, though *in situ* esterification reaction conditions result in some degradation of the C12 SAM, due to the prolonged ethanolic HCl exposure, we conclude that the reaction selectively catalyzes the reaction of MUDA molecules without significantly disturbing unfunctionalized molecules. The slight degradation observed could be decreased by optimizing the *in situ* esterification reaction conditions, minimizing the time required to react the MUDA SAM. In turn, this would minimize the amount of time any SAM would need to be exposed to ethanolic solution, and thus reduce the degradation of unfunctionalized portions of the film. A 24 h reaction is *not* necessary to esterify a MUDA SAM; this length of exposure was chosen in order to give ample time for the reaction to reach completion. Furthermore, catalysts that promote esterification could be used to reduce the amount of time required to esterify the SAM fully.[84−86] For example, Naik and co-workers[86] were able to esterify, within 15 min, various carboxylic acids with ~93% efficiency using catalytic amounts of tetrabutylammonium tribromide. Both efficiency and kinetics could be further improved by using a dehydrating agent, or other special techniques for the removal of water, which under these conditions hydrolyze the ester.

To establish the susceptibility of unfunctionalized SAMs to molecular exchange caused by *in situ* esterification, both pristine and treated C12 SAMs were exposed to $C12_{d25}$ solutions. Displacement by $C12_{d25}$ molecules would cause a decrease in the intensity of the C−H absorptions in the IRRAS spectra. Figure 6c shows the IRRAS spectrum of the previously treated C12 SAM from Figure 6b after exposure to 1.0 mM $C12_{d25}$ solution. The symmetric and asymmetric methyl absorptions at 2965 and 2878 cm^{-1}, respectively, further decreased in intensity (4 ± 1%) upon exposure to the solution. Once again, similar results were obtained when a pristine untreated C12 SAM was exposed to the 1.0 mM $C12_{d25}$ solution (results not shown). These results show that *in situ* esterification does *not* promote molecular exchange reactions in unfunctionalized molecules, and that the observed molecular exchange is similar to that of an untreated C12 SAM.

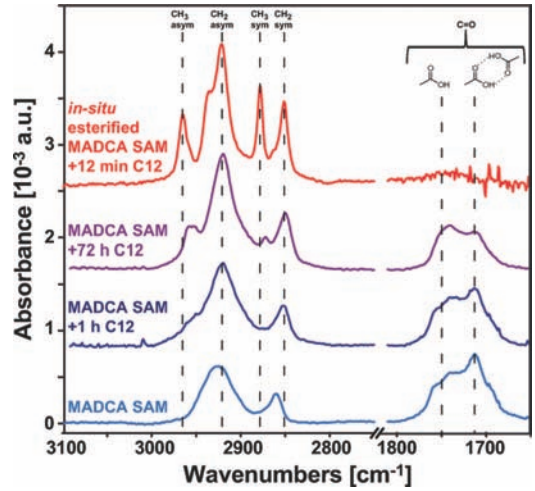

Figure 7. (a) Representative IRRAS spectrum of 3-mercapto-1-adamantanecarboxylic acid (MADCA) SAM. (b) The resulting spectra after (b) 1 h and (c) 72 h exposure to 1.0 mM *n*-dodecanethiol (C12) solution. (d) The spectrum of an *in situ* esterified MADCA SAM after 1 h exposure to 1.0 mM C12 solution. The disappearance of the carbonyl stretches in the *in situ* esterified MADCA SAM spectrum after the 12 min exposure indicates that complete molecular exchange was achieved.

In situ esterification is by no means unique to MUDA SAMs and was also used here to displace MADCA SAMs, a carboxyl-functionalized version of AD. Since MADCA is structurally very different from MUDA (Scheme 2), the ability to apply this methodology to both molecules indicates that our approach is generalizable. Figure 7a (light blue) shows a typical IRRAS spectrum of a pristine MADCA SAM, which has two strong absorptions, at 2926 and 2860 cm^{-1}, attributed to the symmetric and asymmetric methylene stretch modes, respectively. The broad peak at 2926 cm^{-1} is asymmetric, with a longer tail on the low energy side, due to the absorption of the two methine groups in the carbon cage (which in AD SAMs appears around 2934 cm^{-1}).[17,18] After further 1 h exposure to 1.0 mM C12 solution, the MADCA SAM spectrum (Figure 7b, blue) showed a slight increase in the symmetric and asymmetric methylene stretch mode intensities. However, the lack of absorption in the methyl regions indicates a lack of molecular exchange. A 71 h exposure to the C12 solution (Figure 7c, purple) resulted in spectra with contributions from both molecules, with peaks at 2879 and 2964 cm^{-1}. However, even after 72 h total exposure to the C12 solution, very little molecular exchange was observed. Comparing the integrated absorption peak areas of the symmetric methyl stretch with that of a pristine C12 SAM indicates that only 6 ± 2% of the MADCA SAM was exchanged. This low degree of molecular exchange relative to MADCA's unfunctionalized counterpart, AD, which readily undergoes complete and rapid molecular exchange indicates the importance of intermolecular interactions in stabilizing SAMs.[16−18]

In contrast, *in situ* esterified MADCA SAMs are much more susceptible to displacement. Figure 7d (red) shows a representative IRRAS spectrum of an *in situ* esterified MADCA SAM after 12 min of exposure to 1.0 mM C12 solution. The spectrum does not contain a carbonyl absorption and has sharp, well-defined absorption peaks corresponding to a well-ordered alkanethiolate SAM (*vide supra*). Although determining the detailed displacement kinetics of the process is beyond the scope of this paper, a larger

(79) Dannenberger, O.; Weiss, K.; Himmel, H. J.; Jager, B.; Buck, M.; Wöll, C. *Thin Solid Films* **1997**, *307*, 183–191.
(80) Yang, G. H.; Amro, N. A.; Starkewolfe, Z. B.; Liu, G. Y. *Langmuir* **2004**, *20*, 3995–4003.
(81) Nuzzo, R. G.; Zegarski, B. R.; Dubois, L. H. *J. Am. Chem. Soc.* **1987**, *109*, 733–740.
(82) Kondoh, H.; Kodama, C.; Nozoye, H. *J. Phys. Chem. B* **1998**, *102*, 2310–2312.
(83) Kondoh, H.; Kodama, C.; Sumida, H.; Nozoye, H. *J. Chem. Phys.* **1999**, *111*, 1175–1184.
(84) Neises, B.; Steglich, W. *Angew. Chem.* **1978**, *17*, 522–524.
(85) Hussain, M. A.; Liebert, T.; Heinze, T. *Macromol. Rapid Commun.* **2004**, *25*, 916–920.
(86) Naik, S.; Kavala, V.; Gopinath, R.; Patel, B. K. *Arkivoc* **2006**, 119–127.

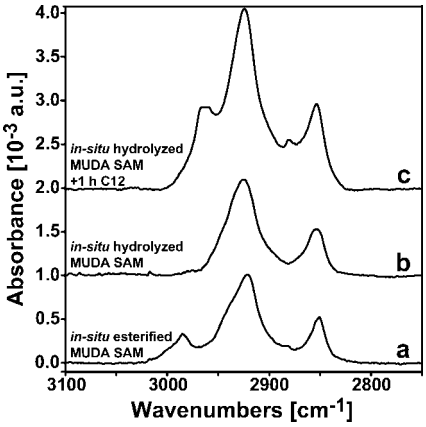

Figure 8. (a) Representative IRRAS spectrum of an *in situ* esterified 11-mercaptoundecanoic acid (MUDA) SAM. (b) The resulting spectrum after hydrolysis, which consists of 24 h exposure to aqueous 5.0 M HCl. (c) The spectrum after 1 h exposure to 1.0 mM *n*-dodecanethiol (C12) solution, showing small amounts of displacement after hydrolysis.

degree of displacement was observed for the *in situ* esterified MADCA SAMs (93 ± 2%), compared to that of the *in situ* esterified MUDA SAMs (86 ± 2%), each after 12 min of exposure to C12 solutions. The ability to switch the reactivity of both MUDA and MADCA SAMs demonstrates that the reaction technique can be made general and can be applied to a range of SAMs that contain carboxyl groups.

3.3. Hydrolysis of *in Situ* Esterified 11-Mercaptoundecanoic Acid SAMs (Step 3, Scheme 1). Esterified SAMs can also be hydrolyzed, returning the switchable surface nearly to its original state. Figure 8a,b shows the spectra of an *in situ* esterified MUDA SAM before and after 24 h *in situ* hydrolysis with 5.0 M HCl aqueous solution. The hydrolysis reaction results in a spectrum that is similar to that of a MUDA SAM, with two peaks corresponding to the symmetric and asymmetric methylene stretches and no evidence of peaks corresponding to the methyl modes. A 1 h exposure to 1.0 mM C12 solution results in spectra with contributions from both MUDA and C12 molecules (Figure 8c), in which the weak methyl absorptions correspond to 7 ± 5% exchange. *In situ* hydrolysis thus substantially neutralizes the promoted exchange observed for *in situ* esterified MUDA SAMs. However, the *in situ* esterification, followed by the hydrolysis reaction, slightly decreases the quality of the original MUDA SAM and results in more molecular exchange (7 ± 5% as compared to 2 ± 1%). Nevertheless, exchange was limited, leaving ~93% of the hydrolyzed molecules in the film. In a complex patterning application, these hydrolyzed molecules could once again serve as controllable sacrificial layers in subsequent patterning steps or modifications.

4. Conclusions and Prospects

We have demonstrated a straightforward and robust strategy for preparing switchable monolayers for use in complex surface patterning applications. The IRRAS and XPS data presented illustrate the effects of *in situ* esterification on the extent of exchange reactions with carboxyl-functionalized alkanethiolates in SAMs. Using MUDA and MADCA SAMs as model systems, with C12 molecules as the exchanging species, *in situ* esterification promoted the molecular exchange reaction (to completion). Without reaction, only very limited molecular exchange (2 ± 1%) took place within the same time frame; this increased somewhat (29 ± 4%) with longer exposures (72 h). The data reveal that *in situ* esterification induces chemical and structural defects that result in partial desorption and increased conformational disorder of the SAMs. Previous studies have shown that the rate and extent of molecular exchange depend on the quality of the SAM, and are both larger for disordered films.[10,21,22,32,33,87] Here, film disorder also appears to play a key role, since well-ordered EMU SAMs deposited from 1.0 mM EMU solutions do *not* show significant molecular exchange, even though they are identical at the molecular level to the *in situ* esterified MUDA SAMs. Thus, the order and defects of the SAM are critical to its stability and properties.

The data also show that the complementary hydrolysis reaction can be employed to quench a partially displaced or patterned surface. Versatile molecular resists for chemical patterning, including soft lithography, need to withstand subsequent chemical and/or physical fabrication steps. Displacement experiments on the pristine MUDA and MADCA SAMs, along with experiments on the hydrolyzed SAMs, show the stability of these films and their applicability as versatile molecular resists when exposed to thiol solutions for relatively short times. The remaining hydrolyzed molecules in the film could act as lateral diffusion barriers to protect the integrity of the patterned features and/or to serve as sacrificial layers for subsequent patterning steps. Typically, resists used in traditional lithographies are sacrificial structures that are used to transfer patterns to the substrate, where exposure to electrons, photons, or ions causes irreversible changes to the film. However, the use of molecules or monolayers as resists, with simple and reversible chemical reactions as the resist exposure mechanism, provides the capability of cycling the resist between its exposed and unexposed states. This may enable the fabrication of complex features with multiple length scales by limiting molecular exchange and/or patterning to different areas of the surface during different patterning steps. Furthermore, by returning the resist to its unexposed state, the resist can serve a dual role, or could even be used to *repair* errors in the functional surface.

This approach should not be limited to carboxyl-terminated SAMs, and could likely be extended to target different functional groups, employing chemical reactions analogous to those used here.[88] The extent of molecular exchange of a single functionality in a multiplexed or multifunctionalized SAM can then be tuned meticulously utilizing this methodology, enabling the patterning of SAMs with precisely tailored compositions and reactivity. Furthermore, this methodology can be used for advanced chemical patterning of functional surfaces that can chemically and biologically interact with their environment at the single-molecule level. These patterned functional surfaces, and this methodology, have potential applications ranging from bioactive/biocompatible surfaces to molecular-sized sensors and electronic components.

Acknowledgment. We acknowledge The Pennsylvania State University Materials Characterization Laboratory and The Pennsylvania State University node of the National Nanotechnology Infrastructure Network for the use of the Kratos XPS system. We thank Dr. Shelley A. Claridge and Mitchell J. Shuster for helpful discussions. We also gratefully acknowledge the National Science Foundation Materials Research and Science Engineering Center (DMR-0820404) and the Army Research Office (W911NF-06-01-02-80) for their support.

JA807648G

(87) Ishida, A.; Majima, T. *Nanotechnology* **1999**, *10*, 308–314.
(88) Al-Rawashdeh, N. A. F.; Azzam, W.; Wöll, C. *Z. Phys. Chem.* **2008**, *222*, 965–978.